Supplementary Material for: The evolution of forecasting for decision-making in dynamic environments

Andrew R. Tilman[1*], Vítor V. Vasconcelos[2,3], Erol Akçay[4], and Joshua B. Plotkin[4]

[1]USDA Forest Service, Northern Research Station, St. Paul, MN, USA
[2]Informatics Institute, University of Amsterdam, Amsterdam, The Netherlands
[3]Institute for Advanced Study, University of Amsterdam, Amsterdam, The Netherlands
[4]Department of Biology, University of Pennsylvania, Philadelphia, PA, USA
[*]Corresponding Author, Email: andrew.tilman@usda.gov

November 29, 2023

In the main text, we describe and analyze an eco-evolutionary model to explore the emergence of forecasting types in dynamically variable environments. The model describes competition among forecasting and myopic types based on mass action kinetics. In other words, the populations of all four states of agents (high- or low-impact strategies and myopic or forecasting types) are well mixed, and interactions occur proportional to frequency. An alternative formulation of the model could consider a hierarchical structure, where forecasting and myopic sub-populations update their strategies within their type, and the sub-populations of cognitive types compete at the group level.

Here, we present the alternative, hierarchical formulation of the model, and we illustrate some of the complex dynamics that this alternative formulation can generate. We perform a change of variables so that the hierarchical and mass-action formulations of the model can be directly compared. This comparison reveals that the primary difference between the models is how the speed of intra-type dynamics responds to the frequency of a type.

Next, we present additional findings for the mass-action model. We illustrate the importance of the discount rate for invasion success, and find that the more weight the future has in decision-making, the more likely forecasters are to invade. We show that forecasting does not entirely resolve the tragedy of the commons: optimal population-level fitness is not necessarily achieved under dominance by forecasting types.

Finally, we introduce an individual-based model that is converges to the model we consider in the main text in the limit of large population size and weak selection.

1 Hierarchical model of forecaster emergence

In this section, we consider an alternative eco-evolutionary dynamic, where there is a hierarchical structure to the system. Forecasters interact only with forecasters, and myopic individuals interact only with myopic individuals for determining strategy dynamics. Then, forecasting and myopic populations compete, based on present payoffs. This hierarchical dynamic leads to a different system of equations governing system dynamics, resulting in some qualitatively distinct outcomes.

We can write the dynamics of this hierarchical system as

$$\dot{y}_L^m = y_L^m(1 - y_L^m)] \, (\pi_L - \pi_H) \tag{1}$$

$$\dot{y}_L^f = y_L^f(1 - y_L^f) \, (f_L - f_H) \tag{2}$$

$$\dot{z}^f = \epsilon_2 z^f (1 - z^f) \left[(y_L^f - y_L^m) \, (\pi_L - \pi_H) - C \right] \tag{3}$$

$$\dot{n} = \epsilon_1 \left[y_L^f z^f + y_L^m (1 - z^f) - n \right]. \tag{4}$$

Notice that $\dot{n}$ also appears in the dynamical equation for the frequency of strategy L among forecasters, this is because forecasters use the current rate of change of the environment to forecast likely future environmental states. Further, notice that C is the cost of forecasting. We assume that both myopic and forecasting agents update their strategies on the same timescale, and that ϵ_2 and ϵ_1 are the relative timescales (as compared to strategy dynamics) of switching between forecasting and myopic, and environmental dynamics, respectively. In sum, we have a four-dimensional system with each variable bound between 0 and 1.

Equation for $\dot{y}_L^m$ Myopic agents update their strategy according to standard replicator dynamics. The payoff difference between the strategies controls the dynamics of switching.

Equation for $\dot{y}_L^f$ Forecasting agents update their strategy based on the present state of the systems as well as based on how the changes in the environment will change future payoffs. Taking into account this future modifies the equation for selection in this case, with payoff forecasts utilized for strategy dynamics.

Equation for $\dot{z}^f$ While we assumed that forecasters update their strategy according to predicted future outcomes, however, forecaster must nonetheless compete with myopic agents in the present. Thus the frequency of forecasters evolves in response to the present payoffs of myopic and forecasting types. The payoff to a myopic agent is

$$y_L^m \pi_L + (1 - y_L^m) \pi_H, \tag{5}$$

and the payoff to forecasting agents is

$$y_L^f \pi_L + (1 - y_L^f) \pi_H - C, \tag{6}$$

Where π_L and π_H are the payoffs of strategies 1 and 2. With these, we can write the payoff difference between forecasting agents and myopic agents as

$$(y_L^f - y_L^m)\pi_L + (1 - y_L^f - 1 + y_L^m)\pi_H - C = (y_L^f - y_L^m)(\pi_L - \pi_H) - C. \tag{7}$$

Intuitively, when strategy L yields higher payoffs than strategy H given the state of the system, forecasters will have higher payoffs than myopic agents if the frequency of strategy L among forecasters, y_L^f, is greater than among myopic agents, y_L^m. Further, since forecasting is costly, the benefits of forecasting must outweigh the cost, C, for forecasters to increase in frequency.

Equation for $\dot{n}$ This is a straightforward modification of the decaying resource environmental feedback from Tilman et al. (2020) with the frequency of strategy L written in terms of our variables.

Comparing the equations for the pairwise interaction (mass action) model with the equations that arise from the hierarchical model provides insight into how the two model structures diverge, and why. In both models, the dynamical equations that govern the frequency of forecasters, z^f, are identical. In both models forecasting and myopic types compete based on present fitness. This does not imply that the invasion processes within the two models are equivalent, however.

In the pairwise interaction model, when forecasters are rare, they mostly interact with myopic individuals, this limits the utility of forecasting, since the forecast is only utilized when interacting with another forecaster. This accounts for the existence of the $z^f(f_L - f_H)$ term in forecaster strategy dynamics under pairwise

interaction; when forecasters are rare, $z^f << 1$, $f_L - f_H$ has a minimal impact on the strategy dynamics of forecasters.

Under the hierarchical model, in contrast, there is no effect of z^f on strategy dynamics for forecasting or myopic types. This is because there are assumed to be two well mixed sub populations where the rate of interaction (and thus strategy dynamics) does not depend on z^f.

Qualitatively, the two models produce distinct invasion dynamics. As shown, invasion under the pairwise interaction model occurs with a long transient, where the frequency of forecasting stays very low. In the long run, a successful invasion by forecasters leads to a new limit cycle.

Under the hierarchical model, forecasters can increase in frequency much more rapidly, since their strategy dynamics are not slowed when they are rare. Figure 1 shows that the hierarchical model produces more complex long run dynamics. For a single set of parameters, a range of long run behaviors are possible. It appears as though there may exist a stable manifold upon which a continuum of neutrally stable orbits occur. This finding, however, is without proof.

2 Relationship between hierarchical and mass-action models

We have described the hierarchical model with a different coordinate system than we used to describe the mass action model in the main text. Here, we perform a change of coordinates on the mass-action model so that we can directly compare the two models, and consider some possible sources of divergence between their results. First, recall the system of equations analyzed in the main text, given by

$$\begin{aligned}
\dot{z}_L^m &= z_L^m z_H^m(\pi_L - \pi_H) + \epsilon_2 z_L^m z_L^f C + \epsilon_2 z_L^m z_H^f(\pi_L - \pi_H + C) \\
\dot{z}_H^m &= -z_H^m z_L^m(\pi_L - \pi_H) + \epsilon_2 z_H^m z_L^f(-\pi_L + \pi_H + C) + \epsilon_2 z_H^m z_H^f C \\
\dot{z}_L^f &= z_L^f z_H^f(f_L - f_H) - \epsilon_2 z_L^f z_L^m C + \epsilon_2 z_L^f z_H^m(\pi_L - \pi_H - C) \\
\dot{z}_H^f &= -z_H^f z_L^f(f_L - f_H) + \epsilon_2 z_H^f z_L^m(-\pi_L + \pi_H - C) - \epsilon_2 z_H^f z_H^m C \\
\dot{n} &= \epsilon_1(z_L^f + z_L^m - n).
\end{aligned}$$

where $\dot{z}_L^m + \dot{z}_H^m + \dot{z}_L^f + \dot{z}_H^f = 1$, denoting the population-wide frequencies of the four strategic types, and $n \in [0, 1]$ is the state of the environment.

With the following transformations, we can perform a change of coordinates to express the mass-action model in the same terms as the hierarchical model.

$$y_L^m = \frac{z_L^m}{z_L^m + z_H^m} \tag{8}$$

$$y_L^f = \frac{z_L^f}{z_L^f + z_H^f} \tag{9}$$

$$z^f = z_L^f + z_H^f \tag{10}$$

$$n = n. \tag{11}$$

With this change of coordinates we can write the dynamical system as

$$\dot{y}_L^m = \frac{\partial y_L^m}{\partial z_L^m}\dot{z}_L^m + \frac{\partial y_L^m}{\partial z_H^m}\dot{z}_H^m \tag{12}$$

$$\dot{y}_L^f = \frac{\partial y_L^f}{\partial z_L^f}\dot{z}_L^f + \frac{\partial y_L^f}{\partial z_H^f}\dot{z}_H^f \tag{13}$$

$$\dot{z}^f = \dot{z}_L^f + \dot{z}_H^f \tag{14}$$

$$\dot{n} = \dot{n}. \tag{15}$$

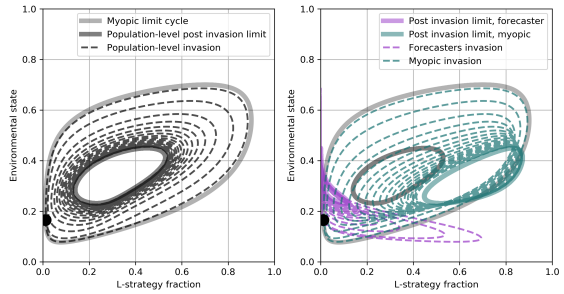

(a) Invasion at $t = 105$

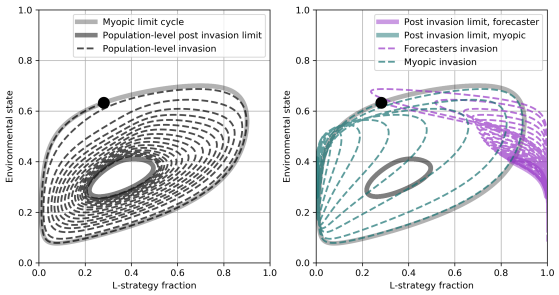

(b) Invasion at $t = 100$

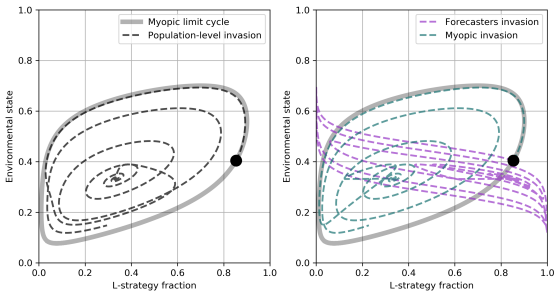

(c) Invasion at $t = 95$

Figure 1: The three panels show that the hierarchical model produces different long-run dynamics given different system states when forecasting types are introduced. In these examples, forecasting types match the frequency of strategy L and H among the myopic types at the time of invasion. The outer light grey loop in the panels is the limit cycle reached by a population of myopic individuals. The dashed lines represent population-level and within type (forecasting or myopic) strategy-environment dynamics during the invasion process. Light red and light blue loops are the long run dynamics of myopic and forecasting types, respectively. Notice that the post-invasion long run dynamics vary depending on the state of the system at the time of invasion. Panels (a) and (b) show subtly different long-orbits post invasion. Panel (c) shows a case where long-run dynamics do not settle into a simple periodic orbit, but rather exhibit periods of environmental (and strategy) stability followed by periods of environmental (and strategy) variability. ($\epsilon_1 = 3/10,\ \epsilon_2 = 1,\ r = 15/100,\ C = 1/100,\ T_1 - R_1 = 2,\ P_1 - S_1 = 4,\ S_0 - P_0 = 1,\ R_0 - T_0 = 3$) The initial frequency of forecasting types is 1/100.

Through collection of terms and substitution of variables, we can write the system in our new coordinate system as

$$\dot{y}_L^m = y_L^m \left(1 - y_L^m\right) \left[(1 - z^f)(\pi_L - \pi_H) + \epsilon_2 z^f (\pi_L - \pi_H)\right] \tag{16}$$

$$\dot{y}_L^f = y_L^f \left(1 - y_L^f\right) \left[z^f (f_L - f_H) + \epsilon_2 (1 - z^f)(\pi_L - \pi_H)\right] \tag{17}$$

$$\dot{z}^f = \epsilon_2 z^f (1 - z^f) \left[(y_L^f - y_L^m)(\pi_L - \pi_H) - C\right] \tag{18}$$

$$\dot{n} = \epsilon_1 \left[y_L^f z^f + y_L^m (1 - z^f) - n\right]. \tag{19}$$

This coordinate systems highlights a few important properties about the system, as constructed. First, the z^f equation shows how forecasting can be favored at the population level. Forecasting types increase in frequency when the forecasting sub-population has a higher frequency of the favored strategy. This is achieved when forecasters foresee that the optimal strategy will soon change, and adopt that strategy earlier and more rapidly than myopic types. Nonetheless, myopic individuals always are at an advantage, as they avoid paying the cost C, of having the ability to forecast.

Second, notice that the forecasting terms, f_L and f_H, only appear in the forecaster strategy equations, and when the prevalence of forecasting is low ($z_L << 1$), little weight is given to these forecasts. Instead, forecasters updating is dominated by the switching of myopic types to forecasters, but this switching is slow and cannot overcome the cost of forecasting, C. Simulations indicate that forecasters need a critical mass to invade, indicating bi-stability. For $\epsilon_2 = 1$, inspection of the dynamical equations near $z^f = 0$ seems to confirm this, forecasting types have the same dynamics as myopic types, but pay a fixed cost C. While forecasting has minimal effect when the frequency of forecasting types is low, we nonetheless have cases where forecasting types can invade.

Third, the strategy dynamic of myopic types is impacted relatively less by changes in the abundance of myopic individuals ($1-z^f$). Within- and cross-type switching is governed by the same process, compensating somewhat for ϵ_2's slowing of strategy dynamics.

3 Additional mass-action model results

3.1 Optimal versus realized long-run fitness

We describe the oscillatory dynamics that occurs under a population composed entirely of myopic types as a 'catastrophe of the commons'. This is because the oscillations that occur lead to further declines in average fitness or profit for the population that would be expected given a standard tragedy of the commons. Forecasting can mitigate or eliminate these oscillations, but when forecasting is costly, environmental stability cannot be attained when forecasting and myopic types compete. Nonetheless, the fitness gains of forecasting are nevertheless largely realized.

However, this does not imply that forecasting types entirely resolve the tragedy of the commons. Figure 2 shows that the optimal fitness that could be attained by a population – by exogenously fixing the frequency of the two strategic types – exceeds the population fitness under forecasting types alone, or under the coexistence of forecasting and myopic types. Therefore, forecasting can resolve a 'catastrophe of the commons' but not the tragedy of the commons. Additional mechanisms are required to resolve problems of cooperation.

3.2 Discounting and the invasion of forecasting types

A key parameter associated with forecasting types is their discount rate. The discount rate determines how much weight forecasters place on the future in decision-making, and so it alters their effective time horizon. Figure 3 shows that as the discount rate decreases, and forecasting types care more about the future, their invasion success rate increases. Lower discount rates are also associated with a small decrease in the long-run frequency of forecasting types after invasion. In contrast to Adamson and Hilker (2020) , we do not find that caring too much about the distant future can backfire and lead to the reemergence of oscillatory dynamics. This is likely because forecasting types update their projections and assessments continuously. Incorrect

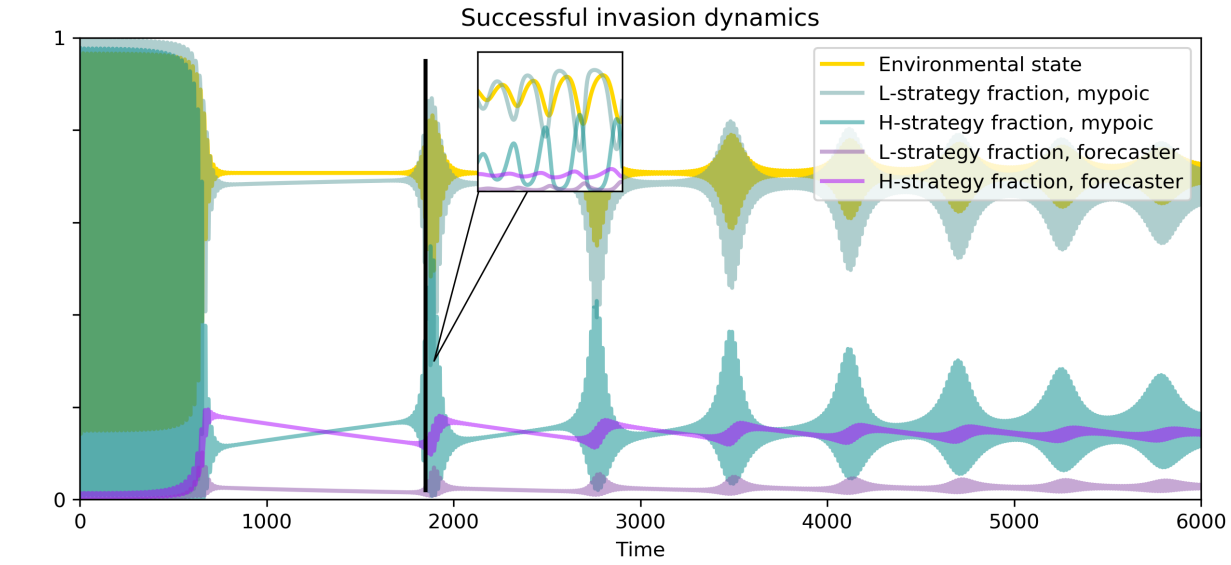

(a)

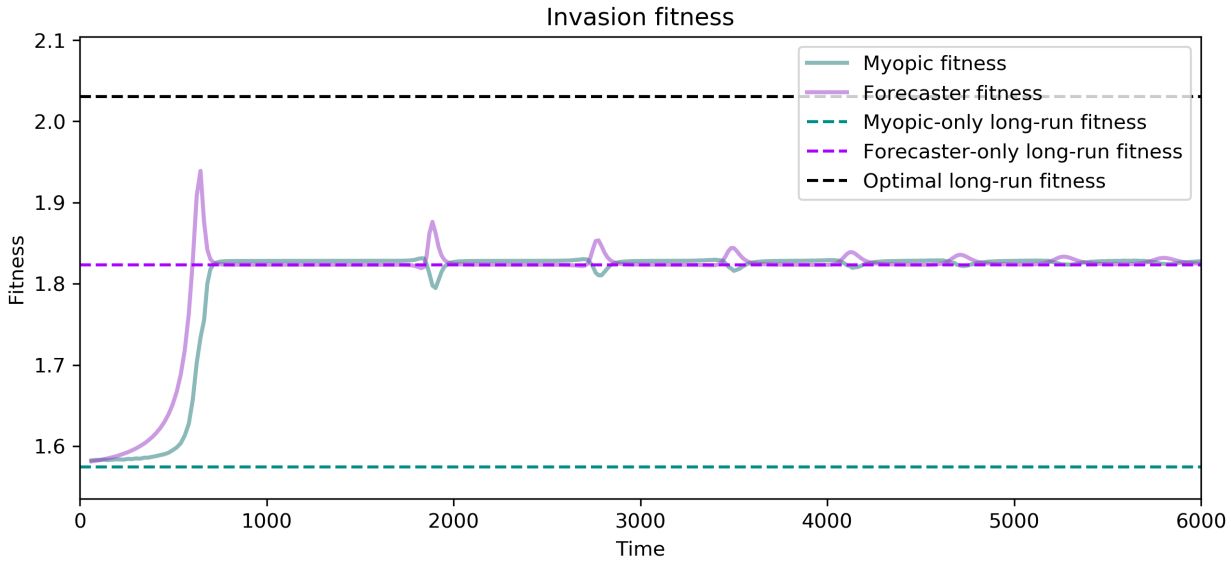

(b)

Figure 2: (a) Forecasting types can invade a resident population of myopic types, leading to coexistence while reducing the amplitude of oscillations. As this example show, a successful invasion of forecasters takes orders of magnitude longer than a single environmental cycle. (b) Dashed lines indicate the long-run fitness that would be attained by populations of purely myopic types, purely forecasting types, or the maximum level of sustained fitness that could be attained at the population level. Solid lines indicate the average fitness of forecasting and myopic sub-populations during the invasion process with both types present. The dynamics of forecasting and myopic types is a social dilemma, forecasting types create public benefits for both forecasting and myopic types. Remarkably, the possible fitness gains of forecasting are attained even in the face of this dilemma. Forecasting mitigates but does not resolve the tragedy of the commons. The optimal long-run population average fitness is greater than the fitness that a population of forecasting types enjoy. $\epsilon_1 = 0.3,\ \epsilon_2 = 0.1,\ r = 0.15,\ C = 0.005,\ R_0 = 8,\ R_1 = 0,\ S_0 = 2,\ S_1 = 0,\ T_0 = 0,\ T_1 = 2,\ P_0 = 0,\ P_1 = 4.$ The initial frequency of forecasting types is 1/70.

predictions about the distant future need to not be adhered to by forecasting types. As environmental trends reverse, so do forecasters predictions.

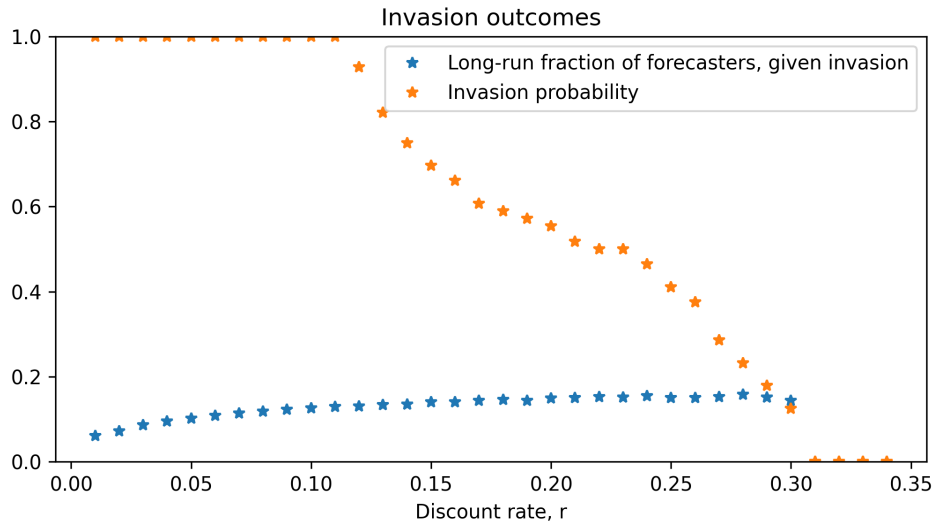

Figure 3: All else being equal, the lower the discount rate, r, the more likely it is that forecasting can invade. This implies that valuing the future more always benefits forecasters, even if they end up putting more decision-making weight on predictions for the far-future that may prove false. However, there is a non-monotonic relationship between the long-run frequency of forecasters and the discount rate that they employ. $(\epsilon_1 = 3/10, \epsilon_2 = 1/10, C = 5/1000, T_1 - R_1 = 2, S_0 - P_0 = 1, R_0 - T_0 = 3, P_1 - S_1 = 4)$ Invasion strategy matched resident. The initial frequency of forecasting types is 1/100.

3.3 Relative fitness under forecasting and myopic populations

The main text focuses on a case where the environmental stability that forecasting can result in increases the average fitness relative to that which would occur under a limit cycle when only myopic agents are present. In this section we explore the question of whether this fitness increase is a universal result of stability, or context dependent. We find that there exist parameter combinations where stability can decrease average fitness relative to the limit cycles that arise under a myopic population. Critically, it is possible to change the payoff functions in a way that does not impact the dynamics of forecasting or myopic types (or the dynamics of the invasion of forecasting types) but does change the relative payoffs of forecasting and myopic types in the long run. This is illustrated in Figures 4-6. Figures 4 and 5 show cases where identical strategy-environment dynamics result in qualitatively distinct fitness outcomes. Figure 6 formalizes this with a parameter sweep across the yellow-shaded region where myopic types experience limit cycles. For points across this region, simulations were run to calculate the average fitness under myopic type limit cycles. This was compared with the fitness that would result from a stable strategy-environment equilibrium that would occur given a population of forecasting types that sufficiently value the future. These payoff differences were used to construct a contour plot that delineates the regions of the parameter space where forecasting increases average fitness (positive values on contours) from those where the stability that forecasting can result in decreases average fitness relative to myopic types (negative values on the contours). Both plots are drawn from parameter combinations which lead to identical dynamics of strategies and the environment, yet distinct fitness outcomes.

3.4 Forecaster invasion dynamics for other payoff regions

In the main text, we focused on the case where $T_1 - R_1 > 0$ and $S_0 - P_0 > 0$ because this region of the parameter space contains cases where cyclic dynamics arise when myopic types dominate. Further, the

conditions for limit cycles in this region of the parameter space have been exhaustively characterized (Tilman et al., 2020). However, there are two other regions of the parameter space where myopic type limit cycles can arise in some cases. Here we explore one of these regions of the parameter space, where $T_1 - R_1 > 0$ but $S_0 - P_0 < 0$. This implies that there is a positive incentive to lead strategy change in a replete environment where everyone in the population follows a low-impact strategy but there is not a positive incentive to switch to the low impact strategy when the environment is in its most degraded state and all individuals are following a high-impact strategy. Figure 7 shows a case within this region of the parameter space where a limit cycle can arise within a bistable regime where an alternative stable state where all individuals following the high-impact strategy is also stable. To test whether the dynamics of invasion in this region of the parameter space are similar to those studied in the main text, we choose an initial condition that converges to a limit cycle under a population of only myopic types. Then we introduce a forecasting subpopulation with a strategy mix that matches the resident myopic population. Figure 8 shows the dynamics of two unsuccessful invasions. In the first, forecasters are introduced at low frequency and despite helping to stabilize the environmental dynamic and increase mean fitness, forecasting types ultimately decline in frequency toward zero. In the second subfigure, forecasting types are introduced at high frequency and nonetheless they still tend toward extinction. Figure 9 show phase portraits for these two cases which illustrate that forecasters drift toward the edge of the state space and are thus unable to react swiftly to changes in conditions that would favor the alternative strategy. We conclude that this region of the parameter space appears to have qualitatively distinct dynamics when forecasting types are introduced to a steady state myopic population, relative to the cases that are highlighted in the main text. While the results in the main text indicate that the success of invasion can depend on when in the limit cycle forecasting types arise, in this case it appears that forecasters fail to invade regardless of initial conditions (though this is without proof).

These alternative dynamical regimes could be important to consider in future studies of alternative modes of decision-making.

4 Individual-based model

In this section, we present an individual-based model that converges to the model we consider in the main text as a limiting case. Consider a well-mixed population of Z individuals interacting in an environmental state, n. Within a timestep τ an agent randomly interacts with another individual in the population and decides whether to adopt that other individual's strategy and (potentially) their decision-making type. In the same timestep, the environment responds to the strategy mixture in the population.

Let Z_L^m, Z_H^m, Z_L^f, and Z_H^f be the number of myopic low-impact strategists, myopic high-impact, forecaster low-impact, and forecaster high-impact strategy individuals in the population, respectively.

4.1 Intra-type strategy change

Myopic individuals will solely consider changing their strategy when they meet other myopic types with a different strategy. They compare the instantaneous payoff of their strategy, π_{current}, with that of the alternative strategy, $\pi_{\text{alternate}}$, and change with a probability given by a sigmoid function,

$$p(x) = \frac{1}{1 + \exp\left[-2\beta x\right]}, \tag{20}$$

as $p(\Pi_{\text{alternate}} - \Pi_{\text{current}})$. Notice that $p(0) = 1/2$, and that this function has the special property that

$$p(x) - p(-x) = \tanh(\beta x) \tag{21}$$

Also, note that β controls the intensity of selection of the best strategy. Alternatively, one can also think of $1/\beta$ as the degree of uncertainty on the payoff difference.

We can write, for a given time t, the probability a myopic individual changes from the low to high impact strategy within a timestep τ, corresponding to a transition, at the population level, from the state $\{Z_L^m, Z_H^m, Z_L^f, Z_H^f, n\}$ at time t to $\{Z_L^m - 1, Z_H^m + 1, Z_L^f, Z_H^f, n'\}$ at time $t + \tau$, as

$$\tau T^{mL\downarrow mH\uparrow} = \tau \frac{Z_L^m}{Z} \frac{Z_H^m}{Z-1} p(\pi_H - \pi_L). \tag{22}$$

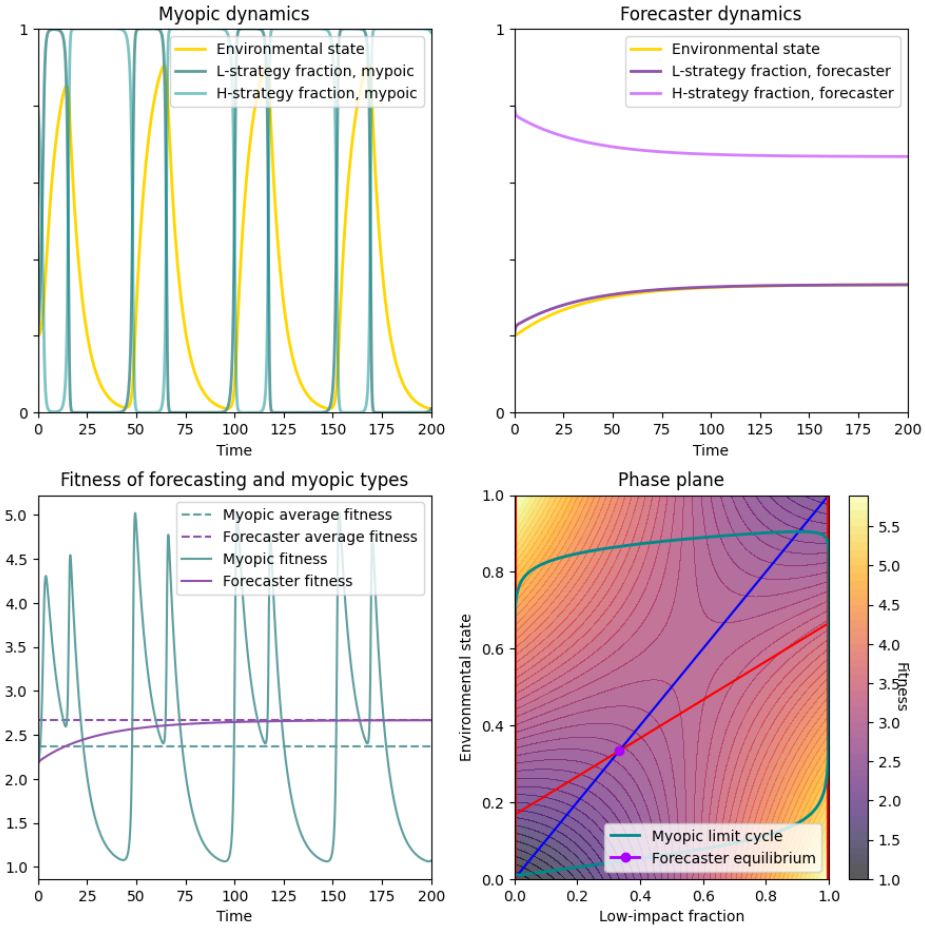

Figure 4: The first two panels illustrate that for these parameter values, a limit-cycle results under myopic types and whereas forecasting types converge to an equilibrium. Panel 3 shows fitness dynamics and long-run averages under forecasting and myopic types. In this case, forecasting types have higher average fitness. The final panel plots the phase plane and nullclines that apply to myopic types. Is shows the limit-cycle that myopic types converge to and the equilibrium point that forecasting types approach. The population fitness landscape is illustrated with a contour plot. ($\epsilon_1 = 15/100,\ r = 5/100,\ C = 5/1000,\ T_1 = 4, R_1 = 2,\ P_1 = 6, S_1 = 1,\ R_0 = 6, T_0 = 2, S_0 = 2, P_0 = 1$)

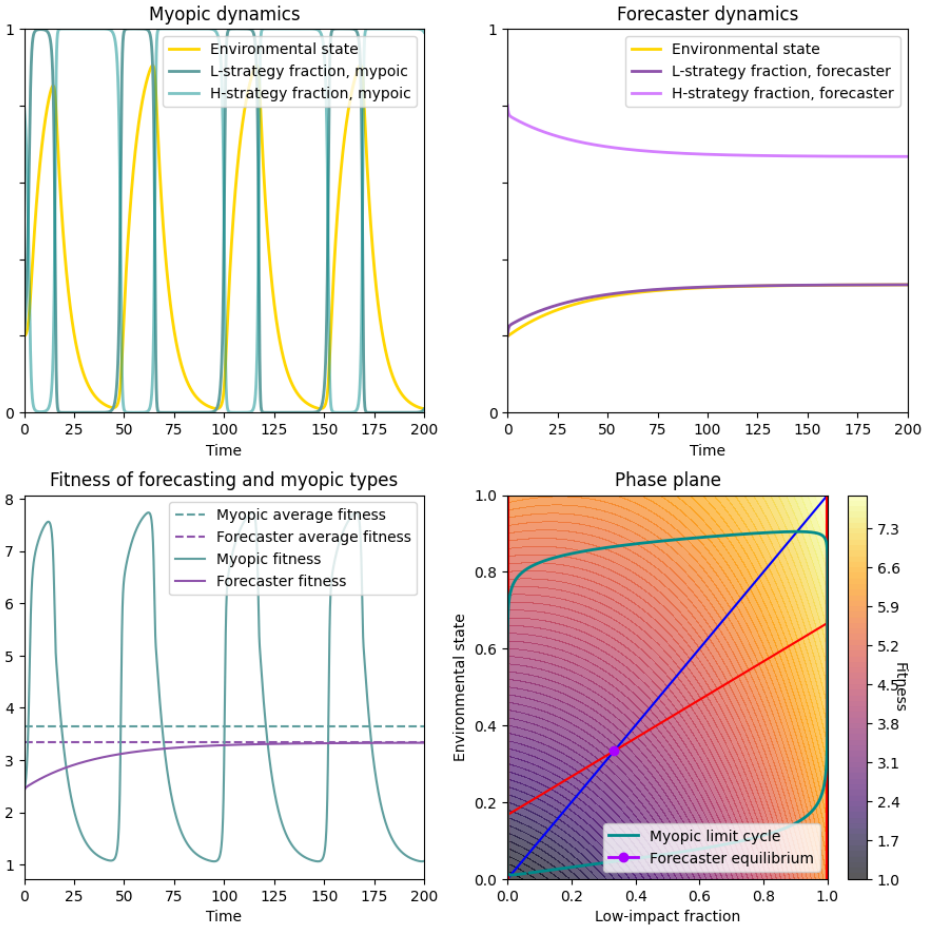

Figure 5: Despite being generated from different parameter values, the first two panels show that the dynamics of forecasting and myopic types are identical to the previous figure. Panel 3 shows the dynamics and long run average of fitness under forecasting and myopic types. In contrast to the previous case, myopic types have higher average fitness than forecasting types. The final panel plots the phase plane and nullclines under only myopic types and shows the population fitness landscape with a contour plot. Relative to the previous figure, the temporal dynamics are identical, and the dynamics of invasion of forecasters would also be identical. However, the fitness landscape is dramatically altered and myopic agents obtain higher average fitness but experience substantial volatility in their payoffs through time. This volatility would reduce their utility under risk aversion. ($\epsilon_1 = 15/100,\ r = 5/100,\ C = 5/1000,\ T_1 = 10, R_1 = 8,\ P_1 = 6, S_1 = 1,\ R_0 = 6, T_0 = 2, S_0 = 2, P_0 = 1$)

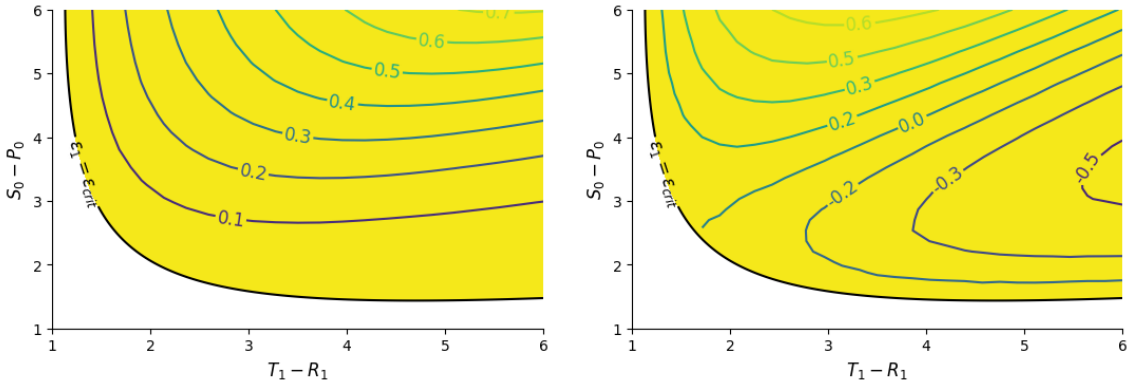

(a) Case where $T_1 = 4, R_1 = 2$

(b) Case where $T_1 = 10, R_1 = 8$

Figure 6: The yellow region denotes the part of the parameter space where cyclic dynamics occur under myopic types ($\epsilon_{crit} < \epsilon_1$), with the boundary illustrated with a black line. The contour plot denotes the difference between fitness under a stable forecaster equilibrium relative to average fitness that results from a myopic populations limit cycle. Positive values on the contours denote regions of the parameter space where forecasting increases average fitness whereas negative values on the contours show where forecasting results in decreased average fitness relative. These two panels are drawn from parameter combination which result in identical dynamics, and differ only in the payoffs population obtain under cycles or stable outcomes. Average fitness under a myopic limit cycle was estimated across the region with cycles by simulating myopic dynamics in the absence of forecasting types for an array of incentive parameters that span the yellow region. Once dynamics relaxed toward the limit cycle, average fitness was estimated over one revolution of the limit cycle. Parameters that hold for both panels are ($\epsilon_1 = 15/100,\ r = 5/100,\ C = 5/1000, P_1 \in [2, 7], S_1 = 1,\ R_0 \in [3, 8], T_0 = 2, S_0 = 2, P_0 = 1$). These parameters imply that $T_1 - R_1 = 2$, $P_1 - S_1 \in [1, 6]$, $R_0 - T_0 \in [1, 6]$, $S_0 - P_0 = 1$ across both plots and therefore the region with cycles under only myopic types and the dynamics of myopic types do not vary across the two sub-plots. However, the relative fitness of myopic types and stabilizing forecasting types is dramatically altered.

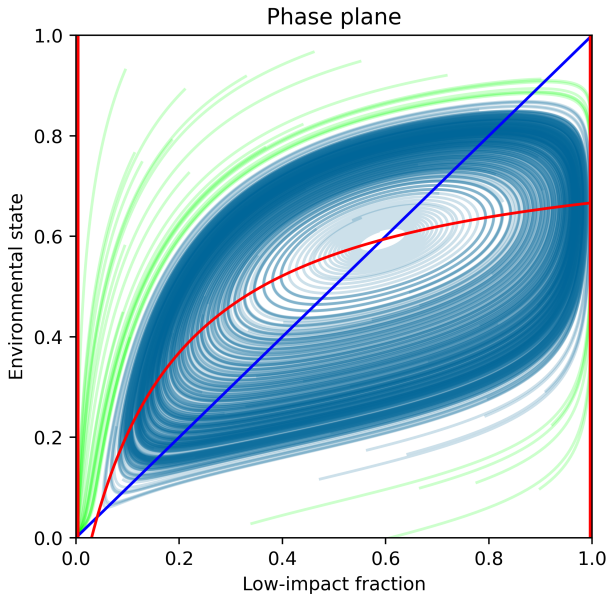

Figure 7: When and are not both positive, it is still possible for cyclic dynamics to result. Here we illustrate a case that illustrates the dynamics of the system in a bistable regime with a limit cycle. Blue solution curves fall within the basin of attraction of the limit cycle and green solution curves fall within the basin of attraction of the edge equilibrium where only the high-impact strategy is followed. The thick blue line is the environmental nullcline, where the environmental state doesn't change, and the red curves are strategy nullclines where the fraction of each strategy is constant. Intersections of these curves are equilibria that may be stable or unstable. ($\epsilon_1 = 25/100,\ T_1 = 6, R_1 = 4,\ P_1 = 4, S_1 = 3,\ R_0 = 6, T_0 = 2, S_0 = 2, P_0 = 17/8$)

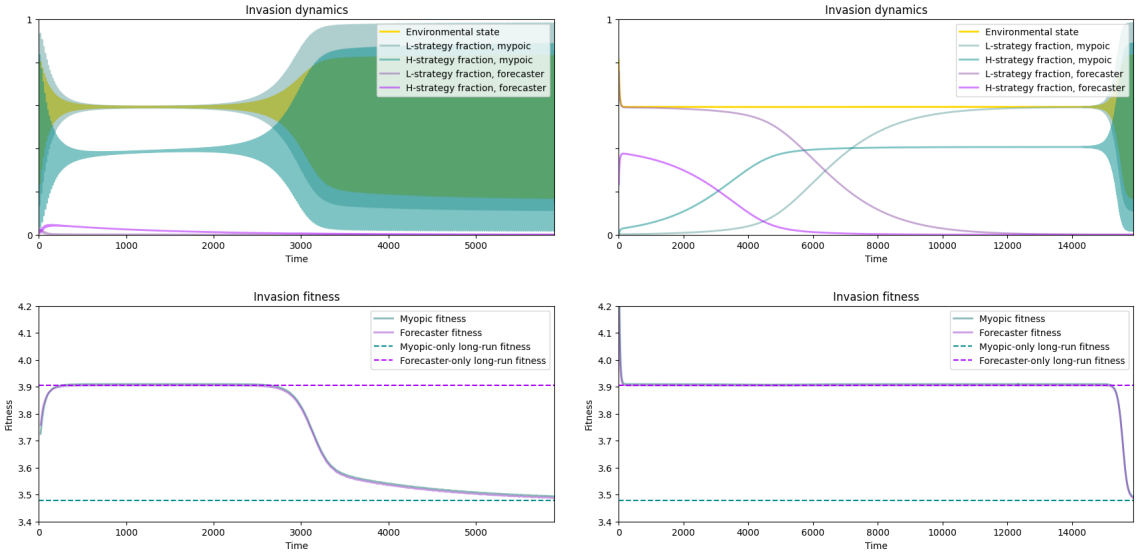

(a) Case where initial forecaster frequency is 1/30

(b) Case where initial forecaster frequency is 99/100

Figure 8: Failed invasions of forecasting types in the region of the parameter space with limit cycles and bistability. Panel (a) shows that when forecasters start relatively rare, they can experience a long transient period with increased environmental stability. Panel (b) shows that even if forecasters comprise nearly all of the population they will eventually be replaced by myopic types. ($\epsilon_1 = 25/100, \epsilon_2 = 15/100,\ r = 5/100,\ C = 5/1000, T_1 = 6, R_1 = 4,\ P_1 = 4, S_1 = 3,\ R_0 = 6,$
$T_0 = 2, S_0 = 2, P_0 = 17/8$)

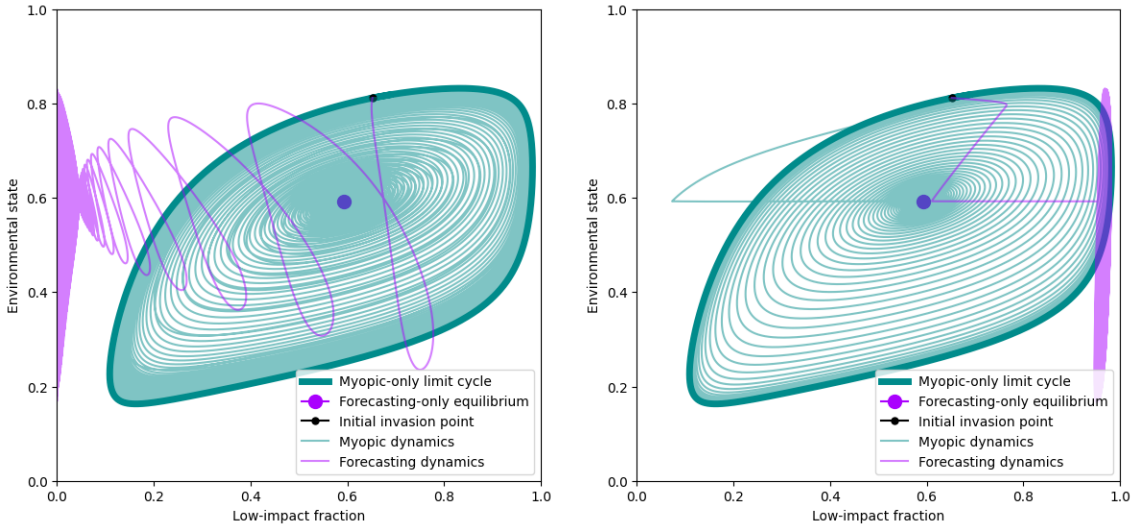

(a) Case where initial forecaster frequency is 1/30

(b) Case where initial forecaster frequency is 99/100

Figure 9: These phase planes provide a different representation of the same dynamics as in the previous figure and show that in this region of the parameter space forecasting and myopic types become polarized in their strategy composition and this polarization seems to preclude the invasion and long-term coexistence of forecasting types. This strategy polarization may correspond to a breakdown of the collective intelligence that forecasting types can otherwise foster. ($\epsilon_1 = 25/100, \epsilon_2 = 15/100,\ r = 5/100,\ C = 5/1000, T_1 = 6, R_1 = 4,\ P_1 = 4, S_1 = 3,\ R_0 = 6,$
$T_0 = 2, S_0 = 2, P_0 = 17/8$)

This can be read as the probability that the individual considering the strategy change is a myopic low-impact one, that they choose an myopic high-impact to compare themselves to, and they do it with the probability p discussed. For simplicity, there is a term that we omit that corresponds to the change in the environment which should read $\delta\left(n' - n(t) - \int_t^{t+\tau} \dot{n}(t')dt'\right)$, where $\delta(x)$ is a Dirac function, which simply states that the environment will evolve to a precise new value in that timestep.

Identically, the probability a myopic individual changes from high to low extraction strategy within timestep τ, corresponding to a transition, at the population level, of the state $\{Z_L^m, Z_H^m, Z_L^f, Z_H^f, n\}$ to $\{Z_L^m + 1, Z_H^m - 1, Z_L^f, Z_H^f, n'\}$, is

$$\tau T^{mH\downarrow mL\uparrow} = \tau \frac{Z_L^m}{Z} \frac{Z_H^m}{Z-1} p(\pi_L - \pi_H). \tag{23}$$

The probability a forecaster changes from high to low or low to high extraction strategy within timestep τ, will depend on discounted payoff forecasts, f. This strategy change corresponds to a transition of the state $\{Z_L^m, Z_H^m, Z_L^f, Z_H^f, n\}$ to $\{Z_L^m, Z_H^m, Z_L^f - 1, Z_H^f + 1, n'\}$ or $\{Z_L^m, Z_H^m, Z_L^f + 1, Z_H^f - 1, n'\}$. The probabilities of these transitions are given by

$$\tau T^{fL\downarrow fH\uparrow} = \tau \frac{Z_L^f}{Z} \frac{Z_H^f}{Z-1} p(f_H - f_L), \tag{24}$$

$$\tau T^{fH\downarrow fL\uparrow} = \tau \frac{Z_L^f}{Z} \frac{Z_H^f}{Z-1} p(f_L - f_H). \tag{25}$$

4.2 Inter-type change

Whereas the dynamics within-types of individuals only considers the possibility of a change of strategy, the dynamics between individuals of different types may or may not also entail strategy change. When a myopic

individual interacts with a forecasting type, they may switch type (and strategy, if necessary) according to a sigmoid function

$$\hat{p}(x) = \frac{1}{1 + \exp\left[-2\gamma x\right]}, \tag{26}$$

so that the strength of selection within types and across types can be varied independently.

We can write the probability a myopic individual with a low impact strategy is replaced by a forecasting individual with a low impact strategy within timestep τ, corresponding to a transition of the state $\{Z_L^m, Z_H^m, Z_L^f, Z_H^f, n\}$ to $\{Z_L^m - 1, Z_H^m, Z_L^f + 1, Z_H^f, n'\}$, as

$$\tau T^{mL\downarrow fL\uparrow} = \tau \frac{Z_L^m Z_L^f}{Z(Z-1)} \hat{p}(-C), \tag{27}$$

because the only payoff difference between these individuals is the extra cost, C, that the forecasting type incurs. Identically for all other replacements

$$\tau T^{mL\downarrow fH\uparrow} = \tau \frac{Z_L^m Z_H^f}{Z(Z-1)} \hat{p}(\pi_H - \pi_L - C), \tag{28}$$

$$\tau T^{mH\downarrow fL\uparrow} = \tau \frac{Z_H^m Z_L^f}{Z(Z-1)} \hat{p}(\pi_L - \pi_H - C), \tag{29}$$

$$\tau T^{mH\downarrow fH\uparrow} = \tau \frac{Z_H^m Z_H^f}{Z(Z-1)} \hat{p}(-C), \tag{30}$$

$$\tau T^{fL\downarrow mL\uparrow} = \tau \frac{Z_L^f Z_L^m}{Z(Z-1)} \hat{p}(C), \tag{31}$$

$$\tau T^{fL\downarrow mH\uparrow} = \tau \frac{Z_L^f Z_H^m}{Z(Z-1)} \hat{p}(\pi_H - \pi_L + C), \tag{32}$$

$$\tau T^{fH\downarrow mL\uparrow} = \tau \frac{Z_H^f Z_L^m}{Z(Z-1)} \hat{p}(\pi_L - \pi_H + C), \text{and} \tag{33}$$

$$\tau T^{fH\downarrow mH\uparrow} = \tau \frac{Z_H^f Z_H^m}{Z(Z-1)} \hat{p}(C). \tag{34}$$

$$\tag{35}$$

4.3 Population state transitions

The state of the system is fully characterized by the number of individuals with each strategy and the environmental state, $i = \{Z_L^m,\ Z_H^m, Z_L^f, Z_H^f\}$ and n, or $x = i, n$. Let us write the transitions that increase (decrease) the number of Z_L^m by one as, $T_i^{mL\pm}$, where we include the subscript x denote that the probability of such a transition will depend on the current state of the population and environment.

$$\tau T_x^{mL+} = \tau(T_x^{mH\downarrow mL\uparrow} + T_x^{fL\downarrow mL\uparrow} + T_x^{fH\downarrow mL\uparrow}), \tag{36}$$

$$\tau T_x^{mL-} = \tau(T_x^{mL\downarrow mH\uparrow} + T_x^{mL\downarrow fL\uparrow} + T_x^{mL\downarrow fH\uparrow}). \tag{37}$$

For the remaining values we can write the same sets of transitions:

$$\tau T_x^{mH+} = \tau(T_x^{mL\downarrow mH\uparrow} + T_x^{fL\downarrow mH\uparrow} + T_x^{fH\downarrow mH\uparrow}), \tag{38}$$

$$\tau T_x^{mH-} = \tau(T_x^{mH\downarrow mL\uparrow} + T_x^{mH\downarrow fL\uparrow} + T_x^{mH\downarrow fH\uparrow}). \tag{39}$$

$$\tau T_x^{fL+} = \tau(T_x^{mL\downarrow fL\uparrow} + T_x^{mH\downarrow fL\uparrow} + T_x^{fH\downarrow fL\uparrow}), \tag{40}$$
$$\tau T_x^{fL-} = \tau(T_x^{fL\downarrow mL\uparrow} + T_x^{fL\downarrow mL\uparrow} + T_x^{fL\downarrow fH\uparrow}). \tag{41}$$

$$\tau T_x^{fH+} = \tau(T_x^{mL\downarrow fH\uparrow} + T_x^{mH\downarrow fH\uparrow} + T_x^{fL\downarrow fH\uparrow}), \tag{42}$$
$$\tau T_x^{fH-} = \tau(T_x^{fH\downarrow mL\uparrow} + T_x^{fH\downarrow mH\uparrow} + T_x^{fH\downarrow fL\uparrow}). \tag{43}$$

For larger population sizes, taking an absolute time scale (e.g., the time scale of the resource dynamics), the time between any two updates, τ is smaller (than at lower population sizes) as the chance that any of the individuals updates increases. Thus, we redefine $\tau \to \tau/Z$ such that τ represents the time it takes an individual to reevaluate their decision (instead of the time step between any two updates). Thus, we write the master-equation for the Markov chain defined by $z = i/Z$ and perform a Kramers-Moyal expansion in $1/Z$, keeping the terms of order $1/Z^2$, which, following the approach of Traulsen et al. (2005) results in a Fokker-Plank equation, whose equivalent Langevin equation is

$$\frac{dz_L^m}{dt'} = T^{mL+}(z,n) - T^{mL-}(z,n) + O(1/Z^{1/2}), \tag{44}$$
$$\frac{dz_H^m}{dt'} = T^{mH+}(z,n) - T^{mH-}(z,n) + O(1/Z^{1/2}), \tag{45}$$
$$\frac{dz_L^f}{dt'} = T^{fL+}(z,n) - T^{fL-}(z,n) + O(1/Z^{1/2}), \text{and} \tag{46}$$
$$\frac{dz_H^f}{dt'} = T^{fH+}(z,n) - T^{fH-}(z,n) + O(1/Z^{1/2}). \tag{47}$$

Now, we can compute these balances of probabilities in order to get an explicit form of the system of ODE's.

$$\begin{aligned} T^{mL+}(z,n) - T^{mL-}(z,n) = {} & T^{mH\downarrow mL\uparrow}(z,n) - T^{mL\downarrow mH\uparrow}(z,n) \\ & + T^{fL\downarrow mL\uparrow}(z,n) - T^{mL\downarrow fL\uparrow}(z,n) \\ & + T^{fH\downarrow mL\uparrow}(z,n) - T^{mL\downarrow fH\uparrow}(z,n), \end{aligned} \tag{48}$$

which has two types of terms, for intra- and inter-type dynamics. The intra-type dynamics are governed by the terms

$$\begin{aligned} T^{mH\downarrow mL\uparrow}(z,n) - T^{mL\downarrow mH\uparrow}(z,n) &= \frac{Z_L^m Z_H^m}{Z(Z-1)} p(\pi_L - \pi_H) - \frac{Z_L^m Z_H^m}{Z(Z-1)} p(\pi_H - \pi_L) \\ &= \frac{Z_L^m Z_H^m}{Z(Z-1)} \left[p(\pi_L - \pi_H) - p(\pi_H - \pi_L) \right] \\ &= \frac{Z}{Z-1} z_L^m z_H^m \left[p(\pi_L - \pi_H) - p(\pi_H - \pi_L) \right] \\ &= \frac{Z}{Z-1} z_L^m z_H^m \tanh\left(\beta(\pi_L - \pi_H)\right), \end{aligned} \tag{49}$$

and the inter-type dynamics are of the form

$$
\begin{aligned}
&T^{fL\downarrow mL\uparrow}(z,n) - T^{mL\downarrow fL\uparrow}(z,n) && (50)\\
+T^{fH\downarrow mL\uparrow}(z,n) - T^{mL\downarrow fH\uparrow}(z,n) \quad &= \frac{Z_L^m Z_L^f}{Z(Z-1)}\hat{p}(C) - \frac{Z_L^m Z_L^f}{Z(Z-1)}\hat{p}(-C)\\
&\quad + \frac{Z_L^m Z_H^f}{Z(Z-1)}\hat{p}(\pi_L - \pi_H + C) - \frac{Z_L^m Z_H^f}{Z(Z-1)}\hat{p}(\pi_H - \pi_L - C)\\
&= \frac{Z}{Z-1}\left[z_L^m z_L^f \tanh(\gamma C) + z_L^m z_H^f \tanh\left(\gamma\left(\pi_L - \pi_H + C\right)\right)\right].
\end{aligned}
$$

If we take the limit as $Z \to \infty$, then consider the limit of weak selection in β, with $\gamma = \beta\epsilon_2$, the higher order terms in Z disappear and tanh() can be approximated linearly, since

$$\tanh(\beta x) = \beta x + O(x^3) \approx \beta x \tag{51}$$

for small values of βx. After re-scaling time so that the β terms drop out of the equations, these limits result in the ODE's we considered in the main text, given by

$$\frac{dz_L^m}{dt} = z_L^m z_H^m(\pi_L - \pi_H) + \epsilon_2 z_L^m z_L^f C + \epsilon_2 z_L^m z_H^f(\pi_L - \pi_H + C). \tag{52}$$

The same arguments applied to the remainder of the strategy dynamical equations also yield the ODE's analyzed in the main text.

4.4 Environmental dynamics

We consider a decaying resource that is emitted as a byproduct of strategies deployed by individuals in the population. We will consider a term, n that corresponds to environmental quality. We want to study a system where when all individuals follow the low-impact strategy, the environment approaches its highest state, $n = 1$, and when all individuals follow a high-impact strategy, the state of the environment declines to $n = 0$. Tilman et al. (2020) show that such a dynamic is mathematically equivalent a re-scaling of the dynamics of pollution emissions. Further, Tilman et al. (2020) show that the dynamics of decaying resources and self-renewing resources are qualitatively equivalent in the context of eco-evolutionary games. Here, we will constrain our analysis to decaying resources since this will lead to fewer model parameters.

We let $n(t)$ be the state of the environment at time t. In a timestep τ/Z, the environment responds to the (constant) current strategy mixture of the population at time t according to

$$n(t + \frac{\tau}{Z}) = n(t) + \frac{\tau}{Z}\epsilon_1\left(\frac{Z_L^f(t) + Z_L^m(t)}{Z} - n(t)\right) \tag{53}$$

so greater numbers of low-impacts strategists leads to an increasing environmental state, with equilibrium points at $n = 1$ when $Z_L^f + Z_L^m = Z$ and $n = 0$ when $Z_L^f + Z_L^m = 0$, as desired. This can be rewritten as

$$\frac{n(t + \frac{\tau}{Z}) - n(t)}{\frac{\tau}{Z}} = \epsilon_1\left(z_L^f(t) + z_L^m(t) - n(t)\right) \tag{54}$$

by rearranging terms and changing from population numbers, Z_L^m to population fractions z_L^m. Following the approach of the previous sections where Z gets large while keeping the average time an individual takes to update, we see that the limit as $Z \to \infty$ is of the form

$$\lim_{\frac{\tau}{Z}\to 0}\frac{n(t + \frac{\tau}{Z}) - n(t)}{\frac{\tau}{Z}} = \frac{dn}{dt}. \tag{55}$$

The equality holds because the expression on the left is the definition of a derivative. This yields an ODE for the dynamics of the environment given by

$$\frac{dn}{dt} = \epsilon_1 \left(z_L^f(t) + z_L^m(t) - n(t) \right) \tag{56}$$

which is the same as the dynamical equation considered in the main text. In summary, we have presented a discrete-time individual-based model that converges to the set of ODEs that we analyze in this paper. This representation gives an explicit micro-level motivation and explanation for the structure of the model analyzed in the main text. To get the dynamics of the individual-based model to converge to the system we study, we made several standard assumptions: that the population size is large, that the update-consideration-rate per individual is independent of population size, and that selection is weak.

References

Adamson, M. W. and Hilker, F. M. (2020). Resource-harvester cycles caused by delayed knowledge of the harvested population state can be dampened by harvester forecasting. *Theoretical Ecology*, 13:425–434.

Tilman, A. R., Plotkin, J., and Akcay, E. (2020). Evolutionary games with environmental feedbacks. *Nature Communications*.

Traulsen, A., Claussen, J. C., and Hauert, C. (2005). Coevolutionary dynamics: from finite to infinite populations. *Physical review letters*, 95(23):238701.